LBL-34077
UC-414

Lawrence Berkeley Laboratory
UNIVERSITY OF CALIFORNIA

Physics Division

Presented at the Rencontres de Physique de La Vallee D'Aoste 1993,
LaThuile, Italy, March 8–13, 1993, and to be published in the Proceedings

Electroweak Physics from DØ

N.A. Roe

May 1993

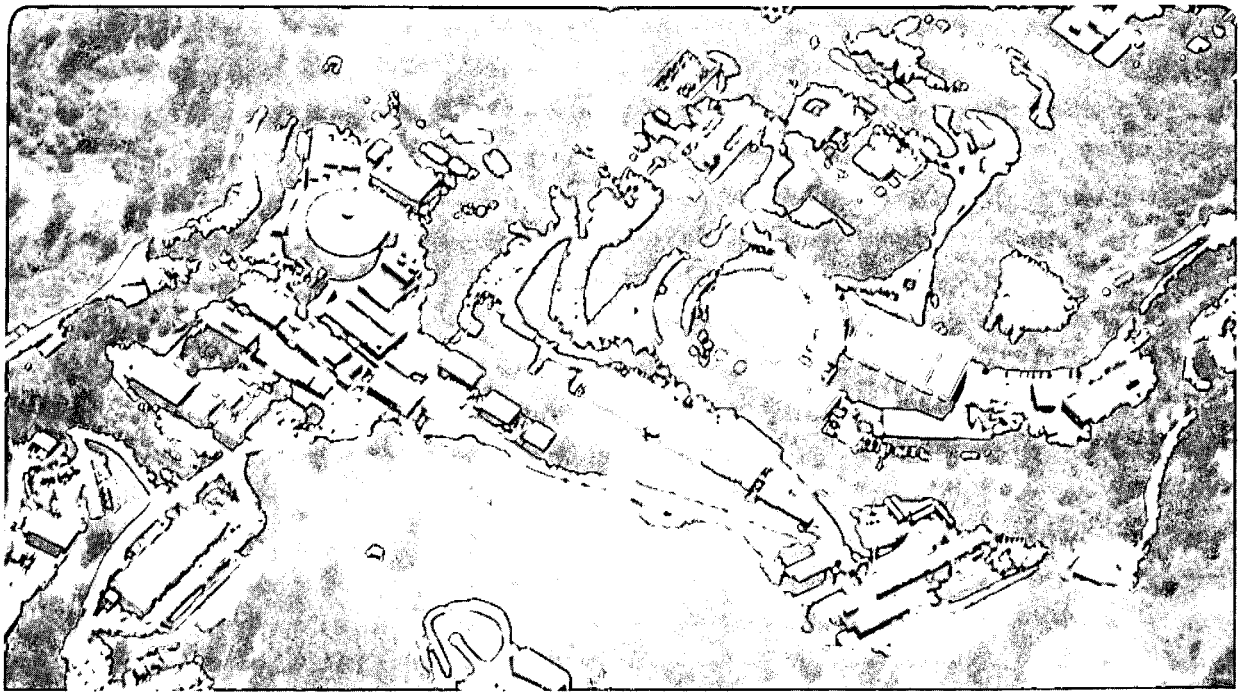

REFERENCE COPY
Does Not
Circulate
Bldg. 50 Library.
LBL-34077
Copy 1

Prepared for the U.S. Department of Energy under Contract Number DE-AC03-76SF00098

DISCLAIMER

This document was prepared as an account of work sponsored by the United States Government. While this document is believed to contain correct information, neither the United States Government nor any agency thereof, nor the Regents of the University of California, nor any of their employees, makes any warranty, express or implied, or assumes any legal responsibility for the accuracy, completeness, or usefulness of any information, apparatus, product, or process disclosed, or represents that its use would not infringe privately owned rights. Reference herein to any specific commercial product, process, or service by its trade name, trademark, manufacturer, or otherwise, does not necessarily constitute or imply its endorsement, recommendation, or favoring by the United States Government or any agency thereof, or the Regents of the University of California. The views and opinions of authors expressed herein do not necessarily state or reflect those of the United States Government or any agency thereof or the Regents of the University of California.

DOE Dist. Cat. UC-414

LBL-34077
May 1993

ELECTROWEAK PHYSICS FROM DØ

Natalie A. Roe

Physics Division
Lawrence Berkeley Laboratory*
University of California
Berkeley, California 94720

Presented at Rencontres de Physique
de La Vallee D'Aoste 1993

March 8-13, 1993

*This work was supported by the Director, Office of Energy Research, Office of High Energy and Nuclear Physics, High Energy Physics Division, of the U.S. Department of Energy under Contract No. DE-AC03-76SF00098.

ELECTROWEAK PHYSICS FROM DØ

Natalie A. Roe
Lawrence Berkeley Laboratory
1 Cyclotron Road, Berkeley, California 94720

Representing the D0 Collaboration[1]

Abstract

The D0 detector was recently commissioned at the Tevatron $p\bar{p}$ collider and is presently taking data. Preliminary results from D0 are presented on properties of the W and Z electroweak gauge bosons, using final states containing electrons and muons.

[1]Universidad de los Andes (Colombia), University of Arizona, Brookhaven National Laboratory, Brown University, University of California, Riverside, Centro Brasiliero de Pesquisas Fisicas (Brazil), CINVESTAV (Mexico), Columbia University, Delhi University (India), Fermilab, Florida State University, University of Hawaii, University of Illinois, Chicago, Indiana University, Iowa State University, Korea University (Korea), Lawrence Berkeley Laboratory, University of Maryland, University of Michigan, Michigan State University, Moscow State University (Russia), New York University, Northeastern University, Northern Illinois University, Northwestern University, University of Notre Dame, Panjab University (India), Institute for High Energy Physics (Russia), Purdue University, Rice University, University of Rochester, CEN Saclay (France), State University of New York, Stony Brook, SSC Laboratory, Tata Institute of Fundamental Research (India), University of Texas, Arlington, Texas A&M University.

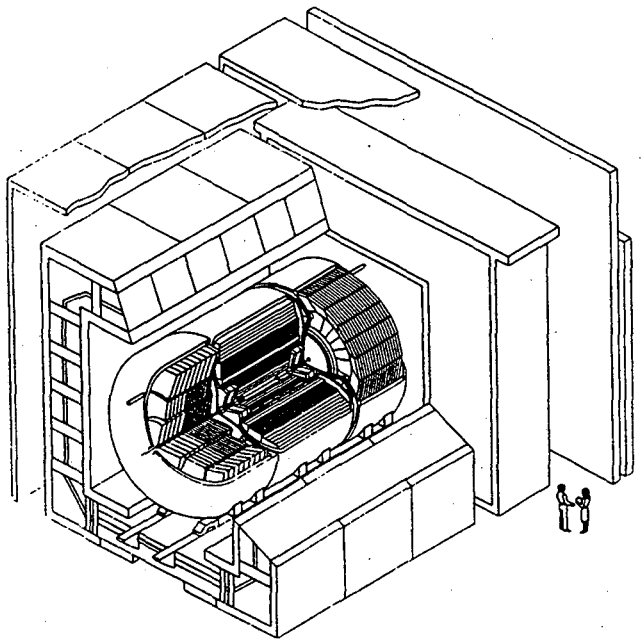

Figure 1: The D0 detector. Three large cryostats contain the uranium–liquid argon calorimeters. Outside the calorimeters are the muon chambers. Tracking chambers are located inside the calorimeters.

1 The D0 Detector

D0 is a large multi-purpose detector operating on the Tevatron $p\bar{p}$ Collider, located at Fermi National Accelerator Laboratory. It features compact, hermetic calorimetry for the detection of electrons, jets and missing transverse energy, and an extensive muon system. The D0 detector has been described in detail elsewhere[1]; see Figure 1 for a cutaway view of the detector. The main features which are relevant for these analyses are the calorimeter and the muon system.

The calorimeter is a uranium–liquid argon sampling detector, contained within a central cryostat and two end cryostats which provide coverage over the range $|\eta| < 4.2$. The electromagnetic section is 21 X_0 deep and has a fractional energy resolution of $15\%/\sqrt{E}$, where E is in GeV, while the hadronic section is 7 - 9 interaction lengths (λ) thick and has a measured fractional energy resolution for pions of $50\%/\sqrt{E}$[2].

The muon system is located outside the calorimeter cryostats. It consists of three superlayers of chambers, with magnetized iron toroids located between the first and second superlayers. Each superlayer has from 4 to 6 layers of proportional wire drift chambers. The magnetic field in the iron toroid is 1.9 Tesla, providing momentum measurement with a design resolution of $\sigma(p)/p = 20\%$, as well as charge discrimination up to 350 GeV/c. The thickness of the calorimeter plus iron toroids varies from 14 λ in the central region to 19 λ in the forward region.

The D0 detector was commissioned during the summer of 1992 and began taking data in August, 1992. At the time of this conference, over 8 pb^{-1} of

data have been logged. The results presented here are preliminary, and based on only part of the data accumulated to date. We anticipate a total data sample in excess of 15 pb^{-1} by the end of the run in June, 1993.

2 W and Z Decays to Muons

The D0 muon trigger has 3 levels. At Level 1, a fast hardware trigger requires at least 2 of 3 muon chamber superlayers to have hits within a wide road, which effectively imposes a minimum transverse momentum requirement of $p_t > 5$ GeV/c. For single and di-muon events the trigger is limited to the pseudo-rapidity region $|\eta| < 1.7$. The Level 1.5 trigger requires all three layers to have hits within a smaller road, imposing a minimum p_t threshold of 7 GeV/c. Finally, the Level 2 trigger imposes software cuts equivalent to those performed off-line, requiring a single muon with $p_t > 15$ GeV/c or two muons each with $p_t > 10$ GeV/c. At Level 2, cosmic rejection cuts are also applied.

Offline, the muon identification code requires a minimum path-length through the magnetized iron toroid of $\int Bdl > 2.0$ T-m, corresponding to a p_t kick of 0.6 GeV/c. The muon must have a good track fit in all three layers, and an impact parameter cut is made requiring $\delta(xy)$ <25 cm and $\delta(rz)$ <15 cm. Additional requirements include a track match with the central drift chamber, a minimum-ionizing signal in the calorimeter, and an isolation cut on calorimeter activity near the muon track.

For $W \rightarrow \mu\nu$ events, a muon with $p_t > 20$ GeV/c is required together with missing transverse energy ($\not{E}_T$) greater than 20 GeV. The resulting transverse mass distribution is shown in Figure 2a. The transverse mass is defined by

$$M_T^2 = 2E_t(e)E_t(\nu)(1 - cos\Delta\phi), \tag{1}$$

where the transverse energy of the neutrino is defined by $E_t(\nu) = \not{E}_T$. The dotted line is the Monte Carlo prediction, absolutely normalized to the integrated luminosity of 4 pb^{-1}. The momentum resolution in the data is not yet optimized, pending completion of alignment and calibration studies. The Monte Carlo data show the transverse mass resolution we expect to achieve; there is also no background included in the Monte Carlo data sample.

For the $Z \rightarrow \mu^+\mu^-$ sample, one muon with $p_t > 20$ GeV/c and a second muon with $p_t > 15$ GeV/c are required. For cosmic rejection, there is an additional requirement that the muons must not be back-to-back. They must satisfy either $\Delta\phi < 160°$ or $\Delta\theta < 170°$, where ϕ and θ are the azimuthal and polar angles, respectively. The invariant mass distribution for the 65 events passing these criteria is shown in Figure 2b, together with the Monte Carlo prediction. Again, the resolution in the data is not as good as that of the Monte Carlo, and no backgrounds are included.

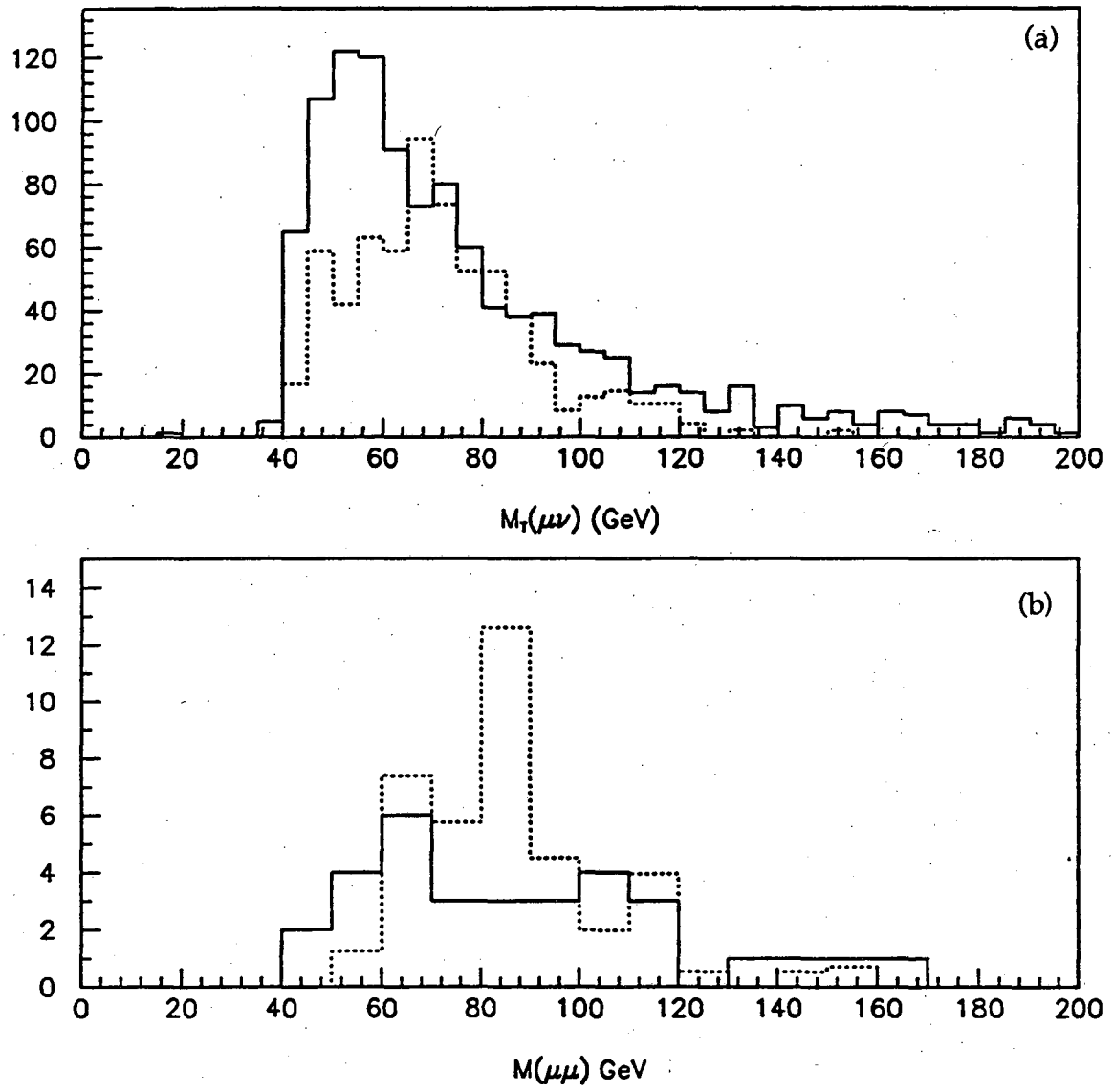

Figure 2: (a) Transverse mass distribution for $W \rightarrow \mu\nu$ events. The solid line is the data (873 events) and the dotted line is the MC prediction. (b) Invariant mass distribution for $Z \rightarrow \mu^+\mu^-$ events. The solid line is the data (65 events) and the dotted line is the Monte Carlo prediction. The Monte Carlo curves are for the design resolution and include no background.

3 W and Z Decays to Electrons

3.1 Electron Identification

The offline electron identification requirements are common to both the cross section and mass analyses, so we present them here. There are four selection criteria which an electromagnetic cluster must satisfy to be defined as an electron:

1) EM/Total Energy > 0.9.
2) Shower Shape χ^2 cut.
3) Isolation < 0.15.
4) Track Match Significance < 10.

The first requirement is simply a cut on the ratio of the electromagnetic energy to the total shower energy. For an electron we expect very little leakage out of the 21 X_o thick electromagnetic section, so this is a rather loose cut. The second requirement uses the 'H-Matrix' technique[3]. In this technique a training sample of electrons is used to compute the mean energy deposited in each calorimeter element along with the correlations to every other element, along with the variance. This is done as a function of energy and pseudo-rapidity. The observed energy deposition is then compared to this correlation matrix and a χ^2 is constructed. The isolation variable, in requirement 3, is defined as the ratio (E(0.4)-EM(0.2))/EM(0.2), where E(0.4) is the total energy inside a cone defined by $\sqrt{\Delta\eta^2 + \Delta\phi^2} < 0.6$ and EM(0.2) is the electromagnetic energy inside a cone of 0.2 in the same units. Finally, we require a good match between the reconstructed track in the central or forward drift chamber and the shower position in the calorimeter. The track match significance variable is defined as $\sqrt{(r \cdot \Delta\phi/\sigma(r \cdot \Delta\phi))^2 + (\Delta z/\sigma(\Delta z))^2}$.

3.2 W and Z Production Cross Section

We have performed a preliminary measurement of the production cross sections for $W^{\pm} \rightarrow e^{\pm}\nu_e$ and $Z^{\circ} \rightarrow e^+e^-$ using a sample of 3.45 pb^{-1}. For W's we require an electron with transverse energy, E_t, greater than 25 GeV, and $\not{E}_T >$ 25 GeV. For Z°'s we require two electrons with E_t >25 GeV. The electrons must be well within the acceptance of the electromagnetic calorimeter, which we have defined here as $|\eta|$ <1.1 or 1.5< $|\eta|$ <3.2. We also exclude the regions in the central calorimeter which are near the small azimuthal gaps between calorimeter modules. These gaps occur every 0.2 radians, and we require that the measured electron position be at least 0.01 radians away, resulting in a 10% loss in efficiency. The combined efficiency for these kinematic and fiducial requirements is 0.51±.04 for W's and 0.42± 0.04 for Z's.

We selected W's and Z's which had satisifed the same trigger. The trigger required one electron with E_t >20 GeV in Level 2 which also passed shower shape and isolation cuts. The trigger efficiency was determined using diagnostic triggers which had a lower E_t requirement or did not impose electron shape and isolation requirements. The trigger efficiency for events

which satisfied the kinematic and fiducial requirements described above was measured to be 0.92± 0.03 for W's and 0.99± 0.01 for Z's.

Finally, the electrons had to satisfy the four standard electron identification requirements described in section 3.1. The combined efficiency of the electron identification cuts for a single electron from W decay was 0.68± 0.05, and for both electrons from Z decay the efficiency was 0.46± 0.07. The greatest source of inefficiency at this time is the track match requirement, and that will improve when detector alignment studies are complete.

The combined efficiency for all selection criteria was 0.32± 0.03 for W's and 0.19± 0.03 for Z's. We applied these criteria to a data set of 3.45± 0.41 pb^{-1}, and obtained a total of 2824 $W \to e\nu$ candidates and 172 $Z \to ee$ candidates. The backgrounds in the W sample were estimated to be $1.0 \pm 0.4\%$ from $W \to \tau\nu$ followed by $\tau \to e\nu\nu$, $1.6 \pm 1\%$ from QCD 2-jet events, and $1.0 \pm 0.5\%$ from $Z \to e^+e^-$ events where one electron was lost. The total background in the W sample was $3.6 \pm 1.2\%$, or 102 events. For Z's a fit was performed to the data, using the sidebands to estimate the background under the peak. The result was a background estimate of 17.7 events, or $10 \pm 3\%$.

Correcting the event yields for the estimated background levels and for inefficiencies due to detector acceptance and event selection criteria, we obtain the following results for the production rates:

$\sigma(p\bar{p} \to W) \cdot \text{Br}(W \to e\nu) = 2.48 \pm 0.05 \pm 0.26 \pm 0.30$ nb, and

$\sigma(p\bar{p} \to Z) \cdot \text{Br}(Z \to e^+e^-) = 0.235 \pm 0.019 \pm 0.040 \pm 0.028$ nb.

The quoted errors are statistical, systematic, and luminosity, respectively. The systematic error includes the uncertainty due to structure functions, and the Z cross section is corrected for the virtual photon terms. At present we are dominated by systematic errors in the efficiency calculations and in the luminosity determination, but we expect to see significant improvement in both as the analyses mature.

The ratio of the above rates is interesting because many common sources of error cancel, including all of the error on the luminosity and part of the errors on the acceptance and event selection efficiency. The ratio can be related to $\Gamma(W)$ in the following way:

$$R \equiv \frac{\sigma \cdot Br(W \to e\nu)}{\sigma \cdot Br(Z \to ee)} = \frac{\Gamma(W \to e\nu)}{\Gamma(W)} \cdot \frac{\Gamma(Z)}{\Gamma(Z \to ee)} \cdot \frac{\sigma(p\bar{p} \to W)}{\sigma(p\bar{p} \to Z)}. \quad (2)$$

From the results quoted above we obtain R=10.55± 0.87 ± 1.07. For the Z width we take the LEP value, $\Gamma(Z) = 2.487 \pm 0.010$ GeV/c^2[4]. The theoretical value for the ratio of W to Z production is $\sigma(p\bar{p} \to W)/\sigma(p\bar{p} \to Z) = 3.23 \pm 0.03$[5]. For the ratio of W and Z electronic decay widths we also take the theoretical value, given by $\Gamma(W \to e\nu)/\Gamma(Z \to ee)) = 2.70 \pm 0.02$[6]. Using equation (2) we obtain the result $\Gamma(W) = 2.06 \pm 0.27$ GeV/c^2.

This measurement of $\Gamma(W)$ can be used to set a limit on non-standard decay modes of the W. In particular, this result can be used to set a limit on the top quark mass which is independent of the top decay modes. In

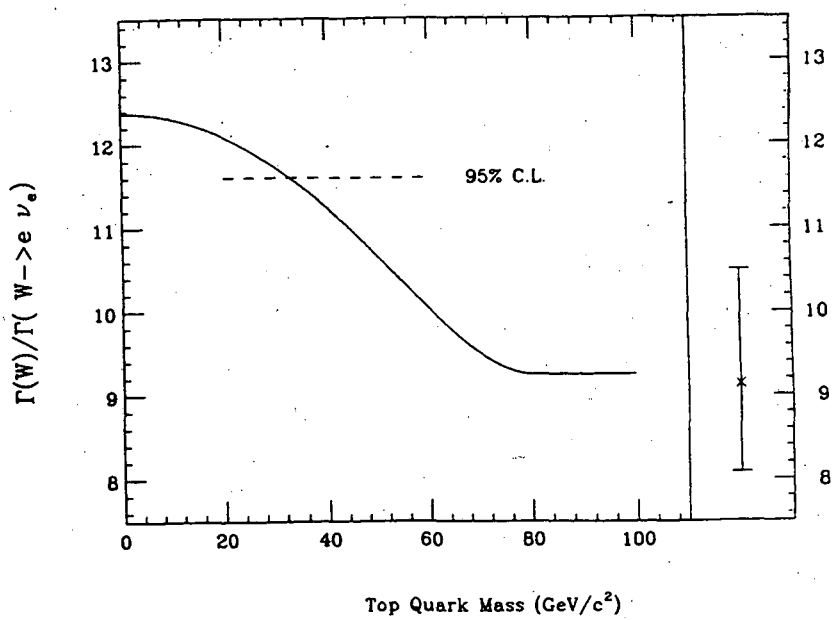

Figure 3: The ratio $\Gamma(W)/\Gamma(W \to e\nu)$ as a function of M_t, together with the preliminary D0 measurement and the 95% C.L. limit.

Figure 3 the ratio $\Gamma(W)/\Gamma(W \to e\nu)$ is plotted as a function of top quark mass, together with the preliminary D0 result $\Gamma(W)/\Gamma(W \to e\nu) = 9.2^{+1.4}_{-1.1}$. (This is obtained from (2) using the LEP value for $\Gamma(Z \to ee)$ of 83.20±0.55 MeV[4].) The 95% C.L. limit is 11.6, corresponding to a top quark mass limit $M_t > 33$ GeV/c^2.

3.3 W and Z Masses

A slightly different data sample was used for the measurement of the W and Z masses. The selection was based on "Express Line" data, a small subset of triggers, rich in events of high interest, which are written directly to disk and immediately analyzed. The trigger requirement for Express Line W candidates was one electromagnetic cluster with $E_t > 20$ GeV and missing transverse energy of at least 20 GeV. The electron candidate was also required to pass the Level 2 software electron filter, which imposed shower shape and isolation requirements. For Z candidates, two electrons were required passing the Level 2 shower-shape and isolation cuts, each with E_t >20 GeV.

At the offline stage the same electron identification cuts were applied as described above in section 3.1. The kinematic requirements of the Level 2 trigger were again imposed using the offline clustering algorithm, which differs from the Level 2 algorithm. In addition, W-candidates were required to satisfy $p_t(W) < 30$ GeV/c. In order to limit the systematic uncertainties in the determination of the masses due to the energy scale, the data samples were restricted to the central calorimeter only. That is, the single electron in W-events and both electrons in Z-events were required to lie within a pseudo-rapidity range $|\eta| \leq 1.1$, and electrons within .01 radians of the azimuthal

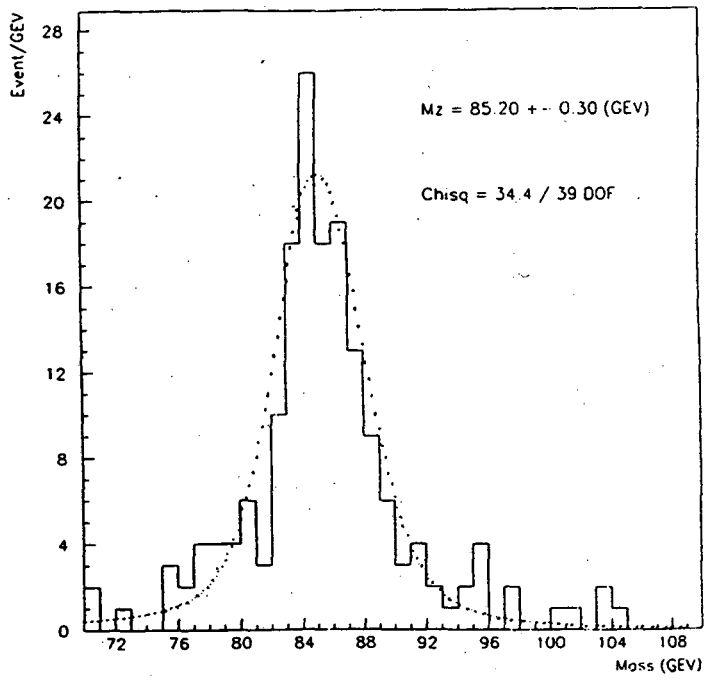

Figure 4: Di-electron invariant mass distribution for Z-candidate events with both electron legs in the central calorimeter.

boundaries between electromagnetic calorimeter modules were removed. This event selection yielded 170 Z^0 candidates and 2904 W candidates.

The mass of the Z^0 is determined by performing an unbinned maximum likelihood fit on the di-electron invariant mass distribution. The invariant mass distribution is fit to a likelihood distribution of the form:

$$f(m_i, \sigma_i, M_Z, \Gamma_Z) = \int_0^\infty \frac{e^{-\beta m'} m'^2}{(m'^2 - M_Z^2)^2 + \frac{m'^4 \Gamma_Z^2}{M_Z^2}} \frac{1}{\sqrt{2\pi}\,\sigma_i} e^{-\frac{(m'-m_i)^2}{2\sigma_i^2}} dm' \quad (3)$$

This is a convolution of the parton luminosity distribution, characterized by the parameter β, and a relativistic Breit-Wigner folded with a Gaussian detector resolution. The width of the Z was fixed in the fit to $\Gamma(Z) = 2.5$ GeV/c^2. The parameter β was taken to be 0.015, as determined from the ISAJET Monte Carlo. Figure 4 shows the di-electron invariant mass distribution for the central calorimeter Z^0-sample. The fitted mass value is 85.2 GeV/c^2, considerably lower than the LEP Z-mass. The question of the absolute energy calibration will be addressed below.

The W-mass is extracted from the transverse mass distribution, where transverse mass is defined as above in section 2. The transverse mass distribution is compared to Monte Carlo distributions generated for different W-masses, taking into account detector effects. The generation of the Monte Carlo events is done in several steps. First, the W-boson momentum vector is generated according to the longitudinal and transverse momentum distributions of Arnold and Kauffmann [7]. A mass is generated according to a relativistic Breit-Wigner line-shape, the W is decayed in its center of mass, and the decay particles are boosted into the lab-frame. Both electron and tau decays of the W are taken into account.

The second step in the generation of the W events is a fast simulation of the DØ detector. One of the important features of this "toy" detector model is that the underlying event is simulated using real minimum bias data. For the results presented here, the underlying event for a W decay has been simulated with a single minimum bias event, chosen according to the total scalar E_t in the event as function of $p_t(W)$. (As the Tevatron luminosity increases, it becomes increasingly important to take into account the effect of multiple interactions, so this model will be refined in the future.) After the underlying event is superimposed on the W-event the $\not{E}_T$ is recalculated and the electron energy and hadronic recoil are smeared according to the resolution as measured in the testbeam and DØ. In the simulation, the hadronic recoil of the W is suppressed by 24% to agree with the results obtained from studies of $\vec{p}_t$ balance in Z^0 events. In the final stage of the event generation the various efficiencies and fiducial cuts are modelled, the most important being the different tracking efficiencies for the central and forward regions (cf. section 3.2).

The Monte Carlo events are generated in a grid of 21 W-masses around a central value in steps of 400 MeV in mass with 10^6 events per mass point. A binned maximum likelihood fit of the Monte Carlo to the transverse mass distribution of the data is then performed in a mass window of 40-90 GeV/c^2. Figure 5a shows the transverse mass distribution and Figure 5b shows the $p_t(W)$ spectrum, with the fit results superimposed. The Monte Carlo fit agrees very well with the data, demonstrating that the calorimeter response is well understood and modelled, up to an overall energy scale factor. It should be noted that it is the ratio M_W/M_Z which is of interest, since M_Z has been very precisely determined by LEP and SLC. In this ratio the overall energy scale cancels out. The preliminary D0 results do obtain a value of M_W/M_Z which is in agreement with the world average value, indicating that the absolute calibration of the energy of the calorimeters is a scale problem rather than an energy offset. However, we have decided to refrain from quoting M_W/M_Z at this point. The energy scale of the calorimeter is under close investigation within the collaboration, and when it has been understood to our satisfaction we are confident that DØ will make a very competitive measurement of the W mass.

4 Conclusions

The DØ detector has been commissioned and is presently taking data at the Tevatron Collider. We have presented preliminary results on W and Z production in both muon and electron channels based on partial data samples. In particular, we have reported preliminary measurements of the W and Z production cross sections with decay into final states containing electrons, and have given a status report on the determination of M_W/M_Z.

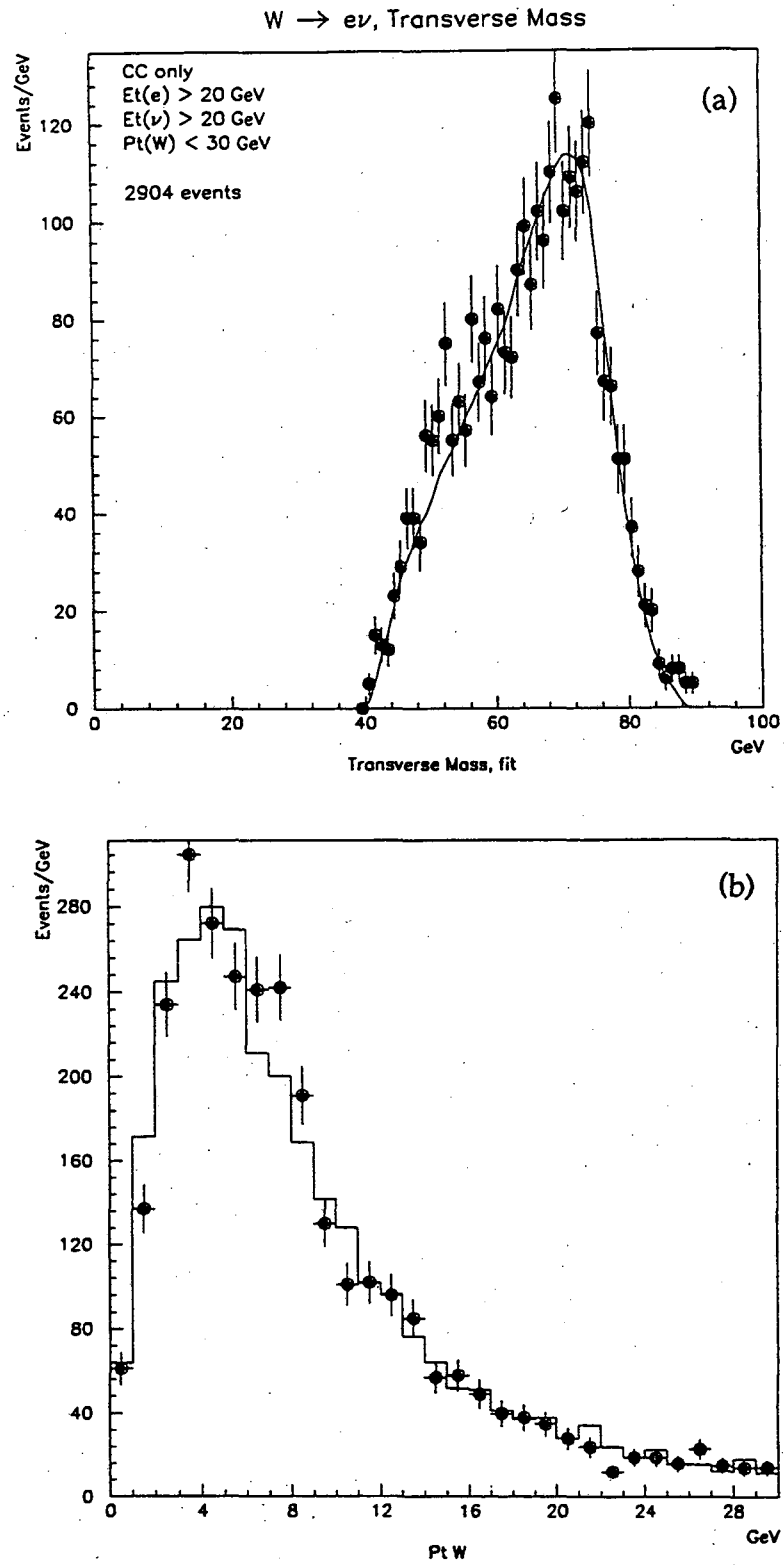

Figure 5: Distribution of the transverse mass (a) and the W transverse momentum of $W \rightarrow e\nu$ events. The points are the data; the solid line is the fit.

5 Acknowledgements

I would like to thank my DØ colleagues for their many contributions to the experiment, and the Fermilab Accelerator Divison for their important role in making our first run a success. In addition I would like to acknowledge Marcel Demarteau for his help with section 3.3.

This work was supported by the Director, Office of Energy Research, Office of Basic Energy Sciences, of the U.S. Department of Energy under Contract No. DE-AC03-76SF00098.

References

[1] S. Abachi, *et. al.*, submitted to NIM.

[2] S. Abachi, *et. al.*, Nucl. Instr. Meth. **A324** 53 (1993).

[3] R. Englemann *et.al.*, Nucl. Instr. Meth **216** 45 (1983).

[4] The LEP collaborations: ALEPH, DELPHI, L3 and OPAL. Phys. Lett. **B276**, 247 (1992).

[5] A.D.Martin,W.J. Stirling, and R.G. Roberts, Phys. Lett. **B228**, 149 (1989).

[6] W.F.L. Hollik, Fortschr. Phys. **38**, 165 (1990).

[7] P. B. Arnold and R. P. Kauffmann, Nuc. Phys. **B349** 381 (1991).

LAWRENCE BERKELEY LABORATORY
UNIVERSITY OF CALIFORNIA
TECHNICAL INFORMATION DEPARTMENT
BERKELEY, CALIFORNIA 94720